


 Cite this: *RSC Adv.*, 2020, **10**, 42557

 Received 6th November 2020
 Accepted 10th November 2020

 DOI: 10.1039/d0ra09459e
rsc.li/rsc-advances

Catalytic coproduction of methanol and glycol in one pot from epoxide, CO_2 , and H_2 †

 Jotheeswari Kothandaraman ^a and David J. Heldebrant ^{ab}

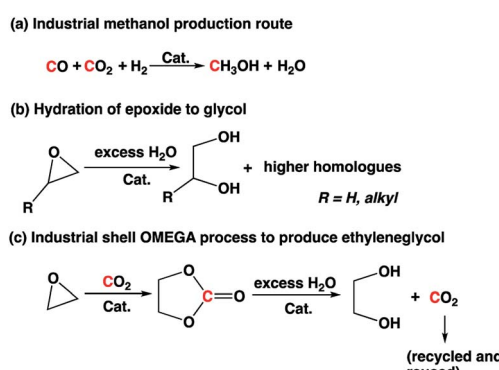
An atom (100%) and energy-efficient approach to coproduce two commodity chemicals, methanol and glycol, has been demonstrated for the first time using H_2 , CO_2 , and epoxide as feeds. A basic medium used for CO_2 capture, polyethylenimine (PEI_{600}), is shown to facilitate the formation of a key reaction intermediate, cyclic carbonates. Upon hydrogenation of cyclic carbonates in the presence of a homogenous Ru-PNP catalyst, a 1 : 1 mixture of methanol and glycol is produced. This approach has been demonstrated in one pot by adding all the required reactants directly or stepwise. The stepwise addition of reactants resulted in good yields (>95% for PG and 84% for methanol) and selectivity of products.

Carbon capture and utilization (CCU) has gained significant attention recently as it is considered as a possible strategy to mitigate anthropogenic CO_2 emissions.¹ CO_2 can be a C_1 source to produce various chemicals such as formic acid, methanol, formate ester, polymers, and cyclic carbonate based on the reaction temperature and starting materials.^{2–4} Among these products, methanol is a commodity chemical that can be used as a feedstock to produce olefins, ethers, fuel blends, acetic acid, and other products.^{2b,5} Industrially, methanol is produced from syngas mixture in the presence of Cu-based catalyst at high temperature and high pressure (Scheme 1).⁶ The reaction byproduct, water, is separated from methanol by distillation

and is not utilized in the process, which lowers the net theoretical atom efficiency to ~73%.

Ethylene glycol and propylene glycol are used as automotive antifreeze, chemical feedstocks for polyester production, and for other miscellaneous applications.^{7,8} Glycols are typically produced by hydrolysis of epoxide in excess water under acidic conditions at high temperature (>150 °C). In addition, the hydrolysis product stream is often contaminated with oligomers of glycols because the product glycol reacts faster with epoxide than water. The use of excess water (~20-fold molar excess) is necessary to reduce the formation of higher homologues, and there is an energy penalty associated with separation of glycol(s) from excess water and oligomers. In the case of ethylene oxide-to-ethylene glycol conversion, a two-step Shell OMEGA process involving first the formation of cyclic carbonate and subsequent hydrolysis of cyclic carbonate to ethylene glycol is practiced industrially to improve the selectivity (Scheme 1).⁹ However, the process still involves an energy-intensive separation process to remove excess water from the product.

We hypothesized that combining the two processes and coproducing methanol and glycol in one pot, the separation associated with excess reagents or byproducts could be avoided, as the byproduct from one reaction is indirectly used as feed for another. Furthermore, the unique reactivity of the captured CO_2 (anionic species) is exploited to ring open the epoxide to form cyclic carbonate, which then is hydrogenated to produce two commodity chemicals at the same time (methanol and glycol) with a theoretical 100% atom efficiency. Approaches for combined methanol and glycol production from epoxide have been explored by others in the literature;¹⁰ however, those processes are not atom-efficient because they use a hydrosilane as a reducing agent, which results in the formation of a stoichiometric amount of chemical waste. Several reports have also been reported on coproduction of methanol and glycols from



Scheme 1 Commercial routes to produce methanol and glycols.

^aEnergy Processes and Materials Division, Pacific Northwest National Laboratory, Richland, Washington 99352, USA. E-mail: david.heldebrant@pnnl.gov

^bDepartment of Chemical Engineering, Washington State University, Pullman, WA 99164, USA

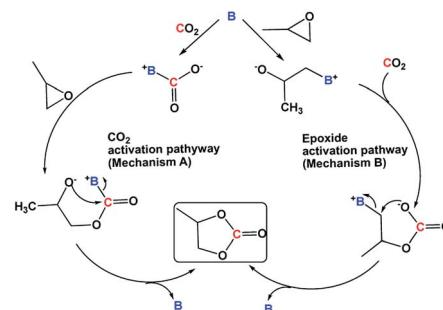
† Electronic supplementary information (ESI) available. See DOI: 10.1039/d0ra09459e



carbonates,^{4 d} but none using CO_2 , epoxide and H_2 directly to the best of our knowledge.

We have previously demonstrated that the amines and amino alcohols used for CO_2 capture also promote the hydrogenation of CO_2 to formate and methanol.^{4 d ,4 g ,11} In this study, we wanted to investigate if such amines and amino alcohols can catalyze the coproduction of methanol and glycol in absence of any additives, by assisting *in situ* formation of cyclic carbonate, an important intermediate that can later be hydrogenated to methanol and glycol. First, monoethanol amine (MEA), the most commonly used post-combustion CO_2 capture solvent was studied as a catalyst for the formation of propylene carbonate (PC) from CO_2 and propylene oxide (PO). MEA produced a very small amount of cyclic carbonate at 110 °C (entry 1, Table 1). When a pre-combustion capture solvent, diethyl ethanol amine (DEEA), was used (entry 2, Table 1), only traces of cyclic carbonate was observed by ^1H NMR experiment. We have previously shown that DBU hexylcarbonate (switchable ionic liquid) catalyzes the reaction of CO_2 to epoxides.^{4 b} However, amidines were not used for this study because they tend to degrade at elevated temperatures under reductive conditions.^{4 d ,4 e}

4-Dimethylaminopyridine (DMAP) was identified as one of the reactive bases that ring open epoxides *via* epoxide activation pathway (Scheme 2).¹² Under our reaction conditions, a cyclic carbonate conversion of 58% was obtained with a good selectivity for PC (entry 3, Table 1). A high boiling polyamine (branched polyethylenimine, PEI₆₀₀) was also screened under the same reaction condition, and a cyclic carbonate conversion of 54% was achieved. Unlike DMAP, which was reported to first



Scheme 2 Proposed reaction mechanisms in the literature.¹³

activate the epoxide, PEI₆₀₀ is expected to activate the CO_2 , first *via* CO_2 activation pathway (Scheme 2) and subsequent nucleophilic attack of the carbanion on the epoxide, opens the ring and cyclizes to carbonate.

Upon the reaction of CO_2 with amines similar to the case of PEI₆₀₀, a carbamic acid species, $[-\text{HN}^+\text{CO}_2^-]$ is first formed, which then exists in equilibrium with carbamate, $[-\text{NH}^+][-\text{NCO}_2^-]$. Therefore, in addition to the CO_2 activation pathway described in Scheme 2, mechanism A, involving carbamic acid intermediate, a competing reaction mechanism involving $[-\text{NH}^+][-\text{NCO}_2^-]$ ion pair is also expected to occur. A DFT calculation of the reaction mechanism for the formation of cyclic carbonate from CO_2 and PO in the presence of DBU hexanol mixture suggested that after the initial activation of CO_2 , the $[\text{DBUH}^+][\text{C}_6\text{H}_{13}\text{OCO}_2^-]$ ion pair ring opens the epoxide (and not the $[\text{C}_6\text{H}_{13}\text{OCO}_2^-]$ anion) and forms PC.^{4 b} Similarly, in the case of PEI₆₀₀, the $[-\text{NH}^+][-\text{NCO}_2^-]$ carbamate ion pair ring opens the epoxide and liberates PC and regenerates $[-\text{NH}^+][-\text{NCO}_2^-]$ carbamate under CO_2 atmosphere.

PEIs are used widely for CO_2 capture studies that are performed both from concentrated sources and air.^{4 c ,4 e ,14} In addition, PEIs are known for their high thermal stability, low volatility, and high amine content. Therefore, PEI₆₀₀ was chosen for further optimization. Lowering the PEI₆₀₀ concentration significantly decreased the cyclic carbonate conversion to 11% (entry 5, Table 1). At room temperature, there was no detectable amount of PC observed, and the PO remained unreacted (entry 6, Table 1). Increasing the temperature to 140 °C resulted in increased cyclic carbonate yield of 97% with a selectivity of >99% (entry 7, Table 1). While superbase and DMAP catalyzed cyclic carbonate formation from epoxide and CO_2 has already been identified in the literature,^{12,13} to the best of our knowledge, high yield production of cyclic carbonate in the presence of polyamine is reported for the first-time in this study.

In the absence of a metal catalyst and only in the presence of PEI₆₀₀, there was no formation of methanol or propylene glycol (PG) (Table 2, entry 1). Several Ru-based catalysts have been identified in the literature for hydrogenation of carbonyl moieties, from which we screened a selected number of catalysts for hydrogenation of *in situ* formed PC.¹⁵ Among the catalysts screened (Table 2, entry 2–4 and Fig. 1), the Ru-PNP pincer catalyst with the aliphatic backbone (catalyst 3) provided good yields for PG (>99%) and methanol (84%), which

Table 1 Propylene carbonate formation from CO_2 and PO^a

Entry	Organocatalyst	Temperature (°C)	PC yield (%)
1	MEA	110	0.2
2	DEEA	110	Traces
3	DMAP	110	58
4	PEI (300 mg)	110	54
5	PEI (100 mg)	110	11
6	PEI (100 mg)	25	0
7	PEI (100 mg)	140	97

^a Reaction conditions: PO = 20 mmol, MEA = 10 mol%, DEEA = 5 mol%, DMAP = 10 mol%, PEI₆₀₀ = 300 mg (entry 4) and 100 mg (entry 5, 6 and 7), THF (5 g, 5.6 mL), initial CO_2 pressure at room temperature = 30 bar, yields were calculated based on the amount of PO (20 mmol) used. 1,3,5-Trimethoxybenzene (TMB) was added as an internal standard.



Table 2 One-pot, one-step vs. two-step CO_2 hydrogenation to methanol and PG^{a,e}

Entry	PO (mmol)	Metal catalyst	CO_2/H_2^b (bar)	PC (%)	PG (%)	CH ₃ OH (%)
						(%)
1 ^c	20 + PEI	—	20/50	96	—	—
2	Entry 7, Table 1	1	60	87	13	—
3	Entry 7, Table 1	2	60	4.8	95	58
4	Entry 7, Table 1	3	60	0	>99	84
5	20	3	20/50	9	54	17
6 ^d	20	3	20/50	9	78	31
7	20 + PEI	3	20/50	12	84	32

^a Reaction conditions: THF = 5 g (5.6 mL), $T = 16$ h, PO = 20 mmol, catalyst = 0.02 mmol, PEI₆₀₀ = 100 mg, $T = 140$ °C, the final reaction mixture from entry 7, Table 1 was hydrogenated in entries 2, 3, and 4 for 16 h. ^b Initial CO_2 and H_2 pressure at room temperature. ^c 24 h. ^d 36 h. ^e Yields were calculated based on the amount of PO (20 mmol) used. TMB was added as an internal standard. No detectable amounts of formate/formyl amides were observed by ¹H NMR in the case of entries 1–6.

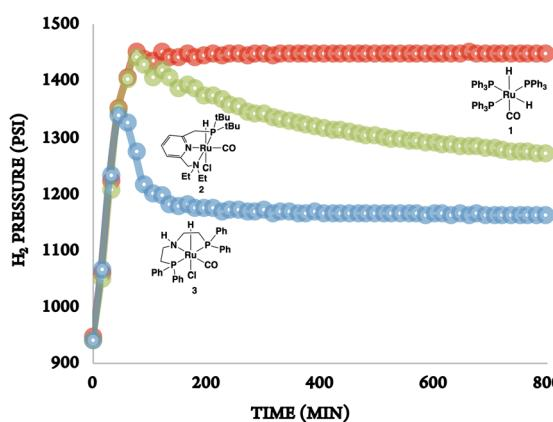


Fig. 1 The rate of hydrogenation of propylene carbonate (in situ formed) in the presence of catalysts 1–3.

corresponds to a turn over number of 1000 based on the amount of glycol formed. No detectable amounts of formate/formyl esters/amides were observed by ¹H NMR (Fig. S4†). Gas chromatographic analysis of the vented gas showed small amounts of CO in addition to H_2 and CO_2 (entry 4, Table 2). Also, subjecting a 1 : 1 mixture of PG and methanol to our experimental reaction conditions (140 °C, 16 h, 60 bar H_2 , THF solvent) and venting resulted in the 1 : 0.9 ratio of glycol and methanol. Therefore, the relatively low methanol yield compared to the PG yield was attributed to (a) methanol loss during depressurization, and (b) decarbonation of methanol.

Next, we attempted combining the steps (a) and (b), which are the PC and PG (and methanol) formation steps, respectively. Even in the absence of PEI₆₀₀, methanol and glycol were formed,

albeit at a lower reaction yield (entry 5, Table 2). Some of the PO remained unreacted (29%), and intermediates such as PC (9%) and formyl esters (11%) were also observed by ¹H NMR experiments. Longer reaction time resulted in improved PG and methanol yields (entry 6, Table 2), and 6.5% of the PO remained unreacted. Interestingly, the concentration of intermediates, PC (9%) and formyl esters (11.5%), produced remained unchanged.

Addition of PEI₆₀₀ increased PG and methanol yields (entry 5 vs. entry 7, Table 2). There was no remaining unreacted PO. However, PC (12%) and formyl esters and amides (11%) were observed by ¹H NMR. The low methanol yields compared to PG in the case of entries 2, 3 and 5–7, Table 1, were due to (a) incomplete hydrogenation of PC to formyl ester intermediates, and (b) side reactions involving CO and methyl formate formations.

The addition of a metal catalyst for the second step required disassembly of the pressurized reactor, which may not be economical for practical application. Therefore, we attempted to add the metal catalyst in step (a) along with PO, PEI₆₀₀, and CO_2 (Table 3). The H_2 was introduced only in step (b). Addition of catalysts 2 or 3 did not change the rate of formation of cyclic carbonate (Fig. S3†). The catalyst 3 formed methanol with good selectivity compared to catalyst 2. The PG and methanol yields of >99% and 82%, respectively, were obtained based on ¹H NMR (Fig. S2†). The calculated yields by GC-MS and ¹H NMR were in agreement. No formyl esters/amides products were observed for both the entries in Table 3.

The use of excess of PEI₆₀₀ (20 times excess, 2 g, nitrogen of PEI : PO ratio of 2), resulted in mostly direct reaction of amine with epoxide and no detectable amount of methanol or cyclic carbonate was observed. Therefore, excess amine cannot be



Table 3 Sequential addition of CO_2 and H_2 ^a

Entry	PO (mmol)	Metal catalyst	PC (%)	PG (%)	CH ₃ OH
					(%)
1	20 + PEI	3	0	>99	82
2	20 + PEI	2	Traces	>99	10

^a THF = 5 g (5.6 mL), total time including cyclic carbonate formation (16 h) and hydrogenation (16 h) steps = 32 h, catalyst = 0.02 mmol, PEI₆₀₀ = 100 mg, initial CO_2 : H_2 = 20 bar: 50 bar (total initial pressure at room temperature = 70 bar) and $T = 140$ °C. Yields were calculated based on the amount of PO (20 mmol) used. TMB was added as an internal standard. No detectable amounts of formate/formyl amides were observed by ¹H NMR.

used for this process, which limits the use of this process for combined capture and conversion, where at least 1 : 1 ratio of amine : epoxide needs to be used.

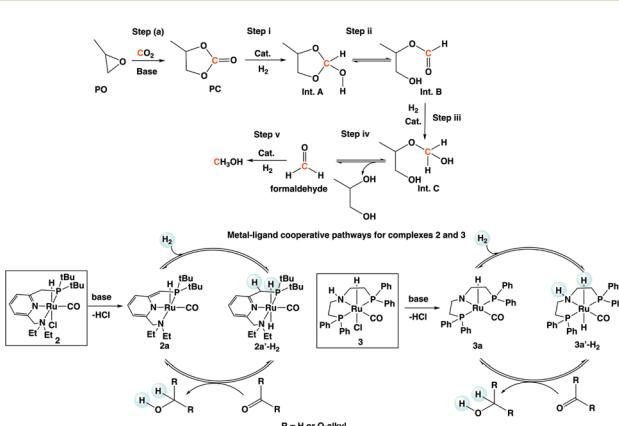
A plausible mechanism for the formation of methanol and glycol is shown in Scheme 3 based on our experimental observation and other reported works in the literature.^{10,15b-d,16} A series of intermediates, such as PC (Step i), Int. B (Step iii), and formaldehyde (Step v), are involved in the reaction mechanism. There are two possible equilibria: (1) Int. A \rightleftharpoons Int. B (Step ii) and (2) Int. C \rightleftharpoons formaldehyde and ethylene glycol (Step iv).

Upon initial activation of pre-catalysts 2 and 3 in the presence of a base, activated catalyst species 2a and 3a are formed (Scheme 3). Heterolytic cleavage of H_2 on 2a and 3a yield dihydride complexes 2a'-H₂ and 3a'-H₂, respectively. The hydrogenation of PC, Int. B, and formaldehyde is catalyzed by dihydride complexes 2a'-H₂ and 3a'-H₂ by a very well investigated metal-ligand cooperation *via* dearomatization (2a)/aromatization (2a'-H₂) or N-H site deprotonation (3a)/protonation (3a'-H₂).^{15a,15c,16a,17} The hydrogenation of each intermediate species (carbonate, formate ester, and

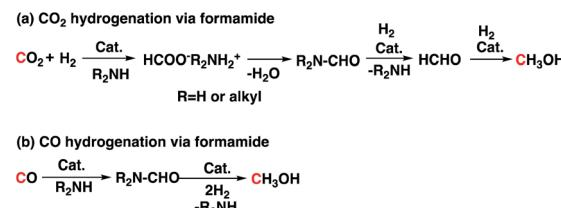
formaldehyde) was already reported in the literature by different groups in the presence of catalysts 2 and 3.^{4e,4f,16a,15c} The reactivity for these intermediates was expected to decrease with decreasing electrophilicity in the following order: formaldehyde > formate ester (Int. B) > PC.^{15d} The protic hydrogen from the "CH₂" and "NH" cooperative sites of the ligands in dihydride complexes 2a'-H₂ and 3a'-H₂ interact with the carbonyl moieties of PC (Step i), Int. B (Step iii), and formaldehyde (Step v) and assist the nucleophilic attack by Ru-H and subsequent formation of Int. A, Int. C, and the final product, methanol.

Catalyst 3 was previously studied for CO_2 and CO hydrogenation to methanol *via* formamide intermediate (Scheme 4). Because we have both CO_2 and H_2 in our reaction, we wondered if this competing reaction is occurring in our reaction medium. To understand this, we performed *operando* magic angle spinning (MAS) ¹³C NMR at 140 °C under 60 bar CO_2 : 3H₂ pressure (Fig. 2).¹⁸ PC was the first intermediate that was formed, and the methanol concentration increased with increasing PC concentration. Formaldehyde was not observed, which suggests that it undergoes hydrogenation readily. There were multiple small signals that appeared between 158–168 ppm, which we attributed to formate esters and amides. Similar to what we previously observed for the experiments in Table 2 (entries 5 and 6, Table 2), the concentration of these broadly assigned formate esters and amides did not change with reaction time. Informed simply by the ¹³C NMR, we could not disregard the direct hydrogenation of CO_2 *via* the formamide pathway. However, the methanol yields never exceeded the glycol yields in any experiments. In addition, methanol was observed in experiments that did not have PEI₆₀₀ (entries 5 and 6, Table 2) and where the formamide could not be formed. Therefore, hydrogenation of CO_2 *via* cyclic carbonate (PC) is likely the major pathway. Unlike the formamide route (reaction (a), Scheme 4), no H_2 is wasted in the formation of water as a byproduct. Ultimately, with H_2 recycling, coproduction could result in a theoretical 100% atom efficiency.

Thermodynamically, the coproduction of methanol and glycol (−32.3 kcal mol^{−1}) is more favorable than the individual reactions of −11.8 kcal mol^{−1} for direct CO_2 hydrogenation to methanol and −20.5 kcal mol^{−1} for hydrolysis of propylene oxide to PG. The energetics for the formation of methanol through CO_2 hydrogenation is compared with the coproduction route in Fig. 3. The presence of alcohols and amines is known to promote the formation of methanol in CO_2 hydrogenation as the reaction proceeds *via* formamide and ester intermediates.^{4e,4f,19} The hydrogenation of ester and formamide are



Scheme 3 Plausible mechanism for the formation of methanol and 1,2-propylene glycol.

Scheme 4 CO_2 and CO hydrogenation *via* formamide intermediate.

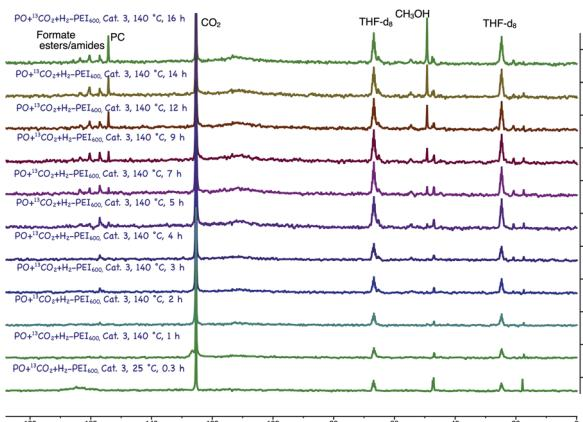


Fig. 2 *In situ* ^{13}C MAS NMR of the one-step, one-pot reaction of PO with $^{13}\text{CO}_2$ and H_2 in the presence of catalyst 3. Reaction conditions: 240 mg propylene oxide + 60 mg PEI₆₀₀ + 2.4 mg catalyst 3 in THF-d₈ (1 mL) at 140 °C. $^{13}\text{CO}_2 : \text{H}_2 = 15$ bar: 45 bar (total initial pressure at room temperature = 60 bar).

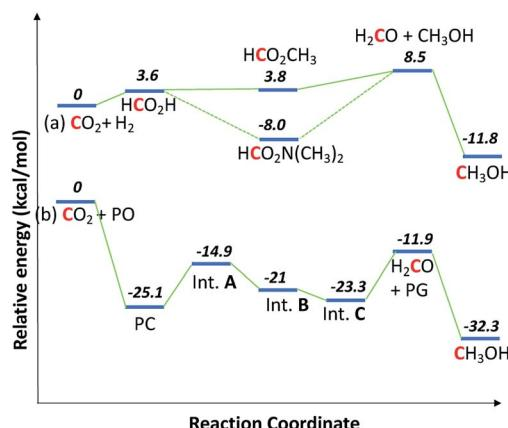


Fig. 3 Energetics for the coproduction of methanol and PG. Relative energies given are enthalpy of reactions, calculated from the method developed by S. W. Benson's group.²¹ (a) and (b) are conventional and coproduction routes, respectively.

the rate limiting steps, which was identified by us and others.^{4d,20} The N-formamide is 11.8 kcal mol⁻¹ more stable than the ester intermediate and, accordingly, the ester is relatively more reactive than the formamide during hydrogenation.

A similar thermodynamic stability study of the intermediates involved in the coproduction process showed that propylene carbonate is the most stable intermediate and thus PC was the main intermediate identified by *operando* ^{13}C NMR (Fig. 2). The formaldehyde formation step is thermodynamically uphill from the starting materials (CO_2 and H_2) in the case of direct CO_2 hydrogenation; consequently, excesses of amines and alcohols are necessary to drive the reaction forward although they further complicate the separation process. On the other hand, in the case of the coproduction approach, a 1 : 1 mixture of glycol and methanol is produced without the need for excess alcohol or amine, therefore easing the separation process.

Conclusions

Two commodity chemicals, methanol and propylene glycol, were produced directly from CO_2 , H_2 , and epoxide for the first time in one pot. PEI₆₀₀ was used for carbon capture and as an organocatalyst for the formation of a cyclic carbonate intermediate that was then hydrogenated in the same pot in the presence of Ru-PNP catalysts to produce methanol and propylene glycol. *Operando* ^{13}C NMR analysis showed the formation of mainly PC and small amounts of ester and amide intermediates under experimental reaction conditions. Unlike the low-temperature (<150 °C) direct CO_2 hydrogenation process in which an excess of alcohols and amines is used, the coproduction approach formed methanol along with glycol in good yields (>95% for PG and 84% for methanol) at 140 °C in the presence of a catalytic amount of amine and the Ru-PNP catalyst. In addition, the coproduction approach reduces the energy-intensive water separation process involved in the individual reactions. Based on this proof of concept study, a convenient separation of methanol and glycol can be achieved by designing a heterogeneous catalyst and solid-supported amine.

Conflicts of interest

There are no conflicts to declare.

Acknowledgements

The authors thank the United States Department of Energy's (DOE's) Office of Science Basic Energy Sciences Early Career Research Program FWP 67038 in the Chemical Sciences, Geosciences, and Biosciences (CSGB) Division for funding. The authors also thank Eric D. Walter and Sarah D. Burton for performing the HT/HP solid-state NMR experiments using EMSL (proposal ID: 51185), a DOE Office of Science user facility sponsored by the Office of Biological and Environmental Research. The Pacific Northwest National Laboratory is operated by Battelle for the DOE.

Notes and references

- (a) A. Al-Mamoori, A. Krishnamurthy, A. A. Rownaghi and F. Rezaei, *Energy Technol.*, 2017, **5**, 834–849; (b) J. Leclaire and D. J. Heldebrant, *Green Chem.*, 2018, **20**, 5058–5081; (c) I. Kim and H. F. Svendsen, *Int. J. Greenhouse Gas Control*, 2011, **5**, 390–395; (d) P. Gabrielli, M. Gazzani and M. Mazzotti, *Ind. Eng. Chem. Res.*, 2020, **59**, 7033–7045.
- (a) J. Klankermayer, S. Wesselbaum, K. Beydoun and W. Leitner, *Angew. Chem., Int. Ed.*, 2016, **55**, 7296–7343; (b) G. A. Olah, A. Goeppert and G. K. S. Prakash, *J. Org. Chem.*, 2009, **74**, 487–498; (c) C. Song, *Catal. Today*, 2006, **115**, 2–32; (d) Q. Liu, L. Wu, R. Jackstell and M. Beller, *Nat. Commun.*, 2015, **6**, 5933.
- (a) M. Bui, C. S. Adjiman, A. Bardow, E. J. Anthony, A. Boston, S. Brown, P. S. Fennell, S. Fuss, A. Galindo, L. A. Hackett, J. P. Hallett, H. J. Herzog, G. Jackson, J. Kemper, S. Krevor, G. C. Maitland, M. Matuszewski, I. S. Metcalfe, C. Petit,



G. Puxty, J. Reimer, D. M. Reiner, E. S. Rubin, S. A. Scott, N. Shah, B. Smit, J. P. M. Trusler, P. Webley, J. Wilcox and N. Mac Dowell, *Energy Environ. Sci.*, 2018, **11**, 1062–1176; (b) B. Smit, A.-H. A. Park and G. Gadikota, *Front. Energy Res.*, 2014, **2**, 55.

4 (a) J. R. Khusnutdinova, J. A. Garg and D. Milstein, *ACS Catal.*, 2015, **5**, 2416–2422; (b) J. Kothandaraman, J. Zhang, V.-A. Glezakou, M. T. Mock and D. J. Heldebrant, *J. CO₂ Util.*, 2019, **32**, 196–201; (c) J. Kothandaraman, A. Goeppert, M. Czaun, G. A. Olah and G. K. S. Prakash, *Green Chem.*, 2016, **18**, 5831–5838; (d) J. Kothandaraman, R. A. Dagle, V. L. Dagle, S. D. Davidson, E. D. Walter, S. D. Burton, D. W. Hoyt and D. J. Heldebrant, *Catal. Sci. Technol.*, 2018, **8**, 5098–5103; (e) J. Kothandaraman, A. Goeppert, M. Czaun, G. A. Olah and G. K. S. Prakash, *J. Am. Chem. Soc.*, 2016, **138**, 778–781; (f) N. M. Rezayee, C. A. Huff and M. S. Sanford, *J. Am. Chem. Soc.*, 2015, **137**, 1028–1031; (g) D. B. Lao, B. R. Galan, J. C. Linehan and D. J. Heldebrant, *Green Chem.*, 2016, **18**, 4871–4874; (h) Y. N. Li, L. N. He, A. H. Liu, X. D. Lang, Z. Z. Yang, B. Yu and C. R. Luan, *Green Chem.*, 2013, **15**, 2825–2829; (i) N. D. McNamara and J. C. Hicks, *ChemSusChem*, 2014, **7**, 1114–1124; (j) J. Su, M. Lu and H. F. Lin, *Green Chem.*, 2015, **17**, 2769–2773; (k) M. Lu, J. Zhang, Y. Yao, J. Sun, Y. Wang and H. Lin, *Green Chem.*, 2018, **20**, 4292–4298; (l) X. L. Du, Z. Jiang, D. S. Su and J. Q. Wang, *ChemSusChem*, 2016, **9**, 322–332; (m) S. Kar, J. Kothandaraman, A. Goeppert and G. K. S. Prakash, *J. CO₂ Util.*, 2018, **23**, 212–218; (n) S. Kar, R. Sen, J. Kothandaraman, A. Goeppert, R. Chowdhury, S. B. Munoz, R. Haiges and G. K. S. Prakash, *J. Am. Chem. Soc.*, 2019, **141**, 3160–3170; (o) C. Reller, M. Poge, A. Lissner and F. O. Mertens, *Environ. Sci. Technol.*, 2014, **48**, 14799–14804; (p) S. Kar, A. Goeppert, J. Kothandaraman and G. K. S. Prakash, *ACS Catal.*, 2017, **7**, 6347–6351.

5 (a) <https://www.methanex.com/about-methanol>; (b) <https://pubchem.ncbi.nlm.nih.gov/compound/Methanol>; (c) G. A. Olah, A. Goeppert and G. K. S. Prakash, *Beyond oil and gas: the methanol economy*, Wiley, Weinheim, 2nd edn, 2009; (d) G. A. Olah, G. K. S. Prakash and A. Goeppert, *J. Am. Chem. Soc.*, 2011, **133**, 12881–12898; (e) J. Kothandaraman, S. Kar, A. Goeppert, R. Sen and G. K. S. Prakash, *Top. Catal.*, 2018, **61**, 542–559; (f) <https://www.methanol.org>.

6 M. Behrens, F. Studt, I. Kasatkin, S. Kuhl, M. Havecker, F. Abild-Pedersen, S. Zander, F. Girgsdies, P. Kurr, B. L. Kniep, M. Tovar, R. W. Fischer, J. K. Norskov and R. Schlogl, *Science*, 2012, **336**, 893–897.

7 M. W. Forkner, J. H. Robson, W. M. Snellings, A. E. Martin, F. H. Murphy and T. E. Parsons, Glycols. In *Kirk Othmer Encyclopedia of Chemical Technology*, John Wiley & Sons, Hoboken, NJ, 2004.

8 (a) <https://pubchem.ncbi.nlm.nih.gov/source/hsdb/174>; (b) <https://pubchem.ncbi.nlm.nih.gov/compound/174>.

9 <https://www.shell.com/business-customers/catalysts-technologies/licensed-technologies/petrochemicals/ethylene-oxide-production/omega-process>.

10 F. D. Bobbink, F. Menoud and P. J. Dyson, *ACS Sustainable Chem. Eng.*, 2018, **6**, 12119–12123.

11 (a) J. Kothandaraman and D. J. Heldebrant, *Green Chem.*, 2020, **22**, 828–834; (b) J. E. Rainbolt, P. K. Koech, C. R. Yonker, F. Zheng, D. Main, M. L. Weaver, J. C. Linehan and D. J. Heldebrant, *Energy Environ. Sci.*, 2011, **4**, 480–484.

12 (a) R. A. Shiels and C. W. Jones, *J. Mol. Catal. A: Chem.*, 2007, **261**, 160–166; (b) J. Sun, W. G. Cheng, Z. F. Yang, J. Q. Wang, T. T. Xu, J. Y. Xin and S. J. Zhang, *Green Chem.*, 2014, **16**, 3071–3078; (c) M. Cokoja, M. E. Wilhelm, M. H. Anthofer, W. A. Herrmann and F. E. Kuhn, *ChemSusChem*, 2015, **8**, 2436–2454.

13 (a) P. P. Pescarmona and M. Taherimehr, *Catal. Sci. Technol.*, 2012, **2**, 2169–2187; (b) G. Fiorani, W. Guo and A. W. Kleij, *Green Chem.*, 2015, **17**, 1375–1389.

14 (a) A. Goeppert, S. Meth, G. K. S. Prakash and G. A. Olah, *Energy Environ. Sci.*, 2010, **3**, 1949–1960; (b) A. Samanta, A. Zhao, G. K. H. Shimizu, P. Sarkar and R. Gupta, *Ind. Eng. Chem. Res.*, 2012, **51**, 1438–1463; (c) X. H. Shen, H. B. Du, R. H. Mullins and R. R. Kommalapati, *Energy Technol.*, 2017, **5**, 822–833; (d) W. Zhang, H. Liu, C. Sun, T. C. Drage and C. E. Snape, *Chem. Eng. Sci.*, 2014, **116**, 306–316.

15 (a) W. Kuriyama, T. Matsumoto, O. Ogata, Y. Ino, K. Aoki, S. Tanaka, K. Ishida, T. Kobayashi, N. Sayo and T. Saito, *Org. Process Res. Dev.*, 2011, **16**, 166–171; (b) S. H. Kim and S. H. Hong, *ACS Catal.*, 2014, **4**, 3630–3636; (c) E. Balaraman, C. Gunanathan, J. Zhang, L. J. Shimon and D. Milstein, *Nat. Chem.*, 2011, **3**, 609–614; (d) J. Pritchard, G. A. Filonenko, R. van Putten, E. J. Hensen and E. A. Pidko, *Chem. Soc. Rev.*, 2015, **44**, 3808–3833; (e) E. Balaraman, B. Gnanaprakasam, L. J. Shimon and D. Milstein, *J. Am. Chem. Soc.*, 2010, **132**, 16756–16758.

16 (a) Z. B. Han, L. C. Rong, J. Wu, L. Zhang, Z. Wang and K. L. Ding, *Angew. Chem., Int. Ed.*, 2012, **51**, 13041–13045; (b) F. Ferretti, F. K. Scharnagl, A. Dall'Anese, R. Jackstell, S. Dastgir and M. Beller, *Catal. Sci. Technol.*, 2019, **9**, 3548–3553; (c) A. Kaithal, M. Holscher and W. Leitner, *Angew. Chem., Int. Ed.*, 2018, **57**, 13449–13453; (d) V. Zubar, Y. Lebedev, L. M. Azofra, L. Cavallo, O. El-Sepelgy and M. Rueping, *Angew. Chem., Int. Ed.*, 2018, **57**, 13439–13443; (e) A. Kumar, T. Janes, N. A. Espinosa-Jalapa and D. Milstein, *Angew. Chem., Int. Ed.*, 2018, **57**, 12076–12080.

17 (a) M. Nielsen, A. Kammer, D. Cozzula, H. Junge, S. Gladiali and M. Beller, *Angew. Chem., Int. Ed.*, 2011, **50**, 9593–9597; (b) D. J. Tindall, M. Menche, M. Schelwies, R. A. Paciello, A. Schafer, P. Comba, F. Rominger, A. S. K. Hashmi and T. Schaub, *Inorg. Chem.*, 2020, **59**, 5099–5115; (c) C. L. Mathis, J. Geary, Y. Ardon, M. S. Reese, M. A. Philliber, R. T. VanderLinden and C. T. Saouma, *J. Am. Chem. Soc.*, 2019, **141**, 14317–14328; (d) S. Kar, M. Rauch, A. Kumar, G. Leitus, Y. Ben-David and D. Milstein, *ACS Catal.*, 2020, **10**, 5511–5515.

18 E. D. Walter, L. Qi, A. Chamas, H. S. Mehta, J. A. Sears, S. L. Scott and D. W. Hoyt, *J. Phys. Chem. C*, 2018, **122**, 8209–8215.



19 (a) M. Everett and D. F. Wass, *Chem. Commun.*, 2017, **53**, 9502–9504; (b) C. A. Huff and M. S. Sanford, *J. Am. Chem. Soc.*, 2011, **133**, 18122–18125; (c) S. Wesselbaum, V. Moha, M. Meuresch, S. Brosinski, K. M. Thenert, J. Kothe, T. V. Stein, U. Englert, M. Holscher, J. Klankermayer and W. Leitner, *Chem. Sci.*, 2015, **6**, 693–704; (d) J. Schneidewind, R. Adam, W. Baumann, R. Jackstell and M. Beller, *Angew. Chem., Int. Ed.*, 2017, **56**, 1890–1893; (e) S. Kar, A. Goeppert and G. K. S. Prakash, *Acc. Chem. Res.*, 2019, **52**, 2892–2903; (f) B. G. Schieweck, P. Jurling-Will and J. Klankermayer, *ACS Catal.*, 2020, **10**, 3890–3894; (g) T. Shimbayashi and K. Fujita, *Tetrahedron*, 2020, **76**, 130946–130974.

20 T. M. Rayder, E. H. Adillon, J. A. Byers and C.-K. Tsung, *Chem*, 2020, **6**, 1–13.

21 E. S. Domalski and E. D. Hearing, *J. Phys. Chem. Ref. Data*, 1993, **22**, 805–1159.

